

Supplementary information

Porphyrin-based metal coordination polymers with self-assembly pathway-dependent properties for photodynamic and photothermal therapy

Yuyang Miao[#], Shibo Lv[#], Daoyuang Zheng, Yuhan Liu, Dapeng Liu*, Fengling Song*

Institute of Molecular Science and Engineering, Institute of Frontier and Interdisciplinary Science. Shandong University, Qingdao, Shandong, 266237, China

dapengliu@sdu.edu.cn

songfl@sdu.edu.cn

Materials and Methods

5,10,15,20-tetrakis(4'-carboxyphenyl)porphyrin (TCPP), $\text{MnCl}_2 \cdot 4\text{H}_2\text{O}$, and NaOH were purchased from Aladdin. Methyl thiazolyl tetrazolium (MTT), 2',7'-dichlorofluorescein (DCFH) and 1,3-diphenylisobenzofuran (DPBF) were purchased from Macklin. The organic solvents used were commercially available without further purification. UV measurements were made on the HITACH UH5300 and fluorescence spectra (FL) were obtained from HITACH F-4700. Nanosecond transient absorption experiments (NTAS) were carried out using an LFP1000 spectrometer at room temperature. A Xe lamp and a picosecond pulsed diode laser (355 nm) were used as the excitation source. The transient absorption signal of thermodynamically stable Mn-TCPP aggregates and intermediate Mn-TCPP aggregates at 460 nm was used for fitting. The optical length in the reported UV-vis, FL and NTAS spectra was 1 cm unless otherwise mentioned. Transition electron microscopy (TEM) images were obtained from Tecnai G2 F20 by the following procedure. A drop of the sample solution was deposited onto the copper grid (230 mesh with carbon film) before dried for overnight. Scanning electron microscope (SEM) images were obtained from HITACH SU8100. All the samples were coated with Au before measurement. Atomic force microscopy (AFM) was performed with Bruker Dimension Lcon. Thermal

gravimetric (TG) analysis profiles were obtained from STA 449 F3 Jupiter. Dynamic light scattering (DLS) measurements were performed using Malvern Nano ZSE. Prior to the DLS measurement, the sample solutions were filtered through 0.45 μm membrane filter. X-ray photoelectron spectroscopy (XPS) was carried out using Thermo Fisher Scientific ESCALAB 250Xi. IR thermal images were obtained from an IR thermal camera (Fluke Tix501). Fluorescence images of cells were taken in a confocal fluorescence microscope (Zeiss LSM 880).

Preparation of Mn-TCPP aggregates

A DMF solution (117 μL) of TCPP (5.4 mM) was added into 10 mL deionized water under 55 $^{\circ}\text{C}$ (328 K) followed by addition of MnCl_2 aqueous solution (70 μL , 42 mM) with stirring at *ca.* 700 rpm. Then aliquots of NaOH aqueous solutions (800 μL in total, $[\text{OH}^-] = 10^{-2}$ M) was added. The process of addition of OH^- solution was monitored by UV spectroscopic method where the resulting mixture was first diluted 15 times with deionized water before measurement. After stirring for *ca.* 1 h at 328 K, the thermodynamically stable Mn-TCPP colloid were obtained. The obtained colloid was then allowed to undergo dialysis against water for 24 h. Finally, the thermodynamically stable aggregates were obtained by addition of 50% DMF/water mixed solution followed by centrifugation under 10000 rpm for 10 min.

The metastable Mn-TCPP aggregates were obtained when the resulting mixture color changed to pink accompanied with the absorption intensity at 415 nm reached maximum. The metastable Mn-TCPP aggregates were centrifugated from the aqueous solution under 12000 rpm for 25min. The metastable Mn-TCPP aggregates were washed with water and DMF, respectively before further characterization.

Dialysis experiment of metastable Mn-TCPP aggregates against deionized water

A solution of metastable Mn-TCPP aggregates in water (7.5×10^{-2} mg/mL, 2 mL) was added into the dialysis bag (molecular weight cut-off: 3500), and then the dialysis bag was put into the large amount of deionized water (25 mL) with stirring at room temperature. The aqueous solution outside of the dialysis bag was monitored with UV-vis absorption

spectroscopic method.

$^1\text{O}_2$ generation of Mn-TCPP aggregates

The singlet oxygen ($^1\text{O}_2$) generation of Mn-TCPP aggregates was evaluated by ROS probe DPBF. In practice, the Mn-TCPP aggregates aqueous dispersion containing DPBF solution (5 mM) were exposed to LED light irradiation (660 nm, 12 mW/cm²). And the absorbance change at 410 nm was recorded in a UV-Vis absorption spectrophotometer.

Photothermal properties of Mn-TCPP aggregates

200 μL of Mn-TCPP aggregates in aqueous solution was dropped on a piece of parafilm. PBS solution was used as a reference sample. Samples were exposed a 637 nm laser irradiation with 200 mW/cm² output. And the surface temperature was recorded using a temperature calibrated infrared camera. And the related thermal images were recorded with a thermal camera (Fluke Tix501).

Cellular ROS detection

The DCFH-DA could be oxidized rapidly by ROS to generate highly fluorescent DCF. Here the DCFH-DA was used as ROS probe to detect the cellular ROS production. In practice, HeLa cells were first incubated in culture dishes for 24 h. Then the cells were treated with 1 mL of DMEM containing 0.1 mg/mL intermediate Mn-TCPP aggregates. After 24 h incubation, 1 mL PBS including DCFH-DA (2.5 μM) was added in each well and cultured for another 20 min. Then the cells were fixed with 4% paraformaldehyde in PBS for 30 min followed by being stained with DAPI for 15 min, and then washed 3 times with PBS. Finally, the cell images were obtained by laser scanning confocal microscope.

Cell viability

Cell viability of PDT/PTT performance was determined by MTT assay. In practice, HeLa cells were incubated in 96-well plates and cultured in a DMEM medium with 10% (v/v) fetal bovine serum (FBS), penicillin (100 U/mL) and streptomycin (100 $\mu\text{g}/\text{mL}$) at 37°C under 5% CO₂ for 24 h. Then the cells were treated with different concentrations of Mn-TCPP aggregates ranging from 110 to 20 $\mu\text{g}/\text{mL}$. After 24 h incubation, the cells in PDT groups were irradiated with LED light (660 nm, 60 mW/cm²) for 20 min. And the cells in

PTT groups were exposed to the LED light (660 nm) at a power density of $60 \text{ mW} \cdot \text{cm}^{-2}$ for 15 min. During the PDT/PTT experiments, the cells in control groups were covered with aluminum foil to remain in the dark. The cells in each well were cultured for another 24 h and then treated with $100 \mu\text{L}$ of 0.5 mg/mL MTT in PBS. After 4 h incubation, the blue formazan crystals were formed. Then DMSO was used to replace the culture medium to dissolve the produced blue formazan crystals and the corresponding absorbance was measured using a microplate reader at a wavelength of 450 nm.

Supplementary figures and tables

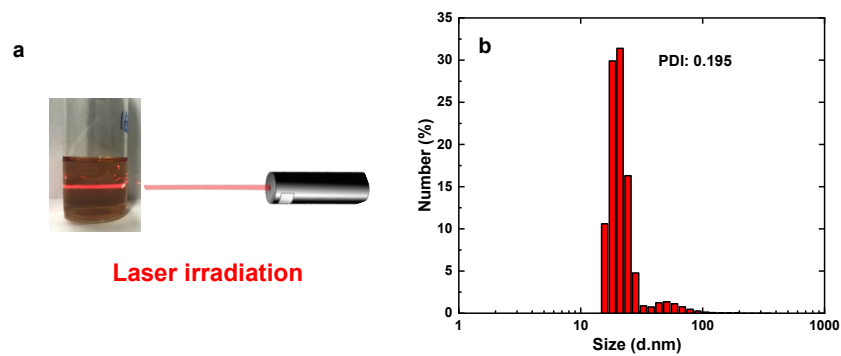


Figure S1. a) Photograph of the prepared Mn-TCPP colloid under laser irradiation. b) DLS profile of the thermodynamically stable Mn-TCPP aggregates.

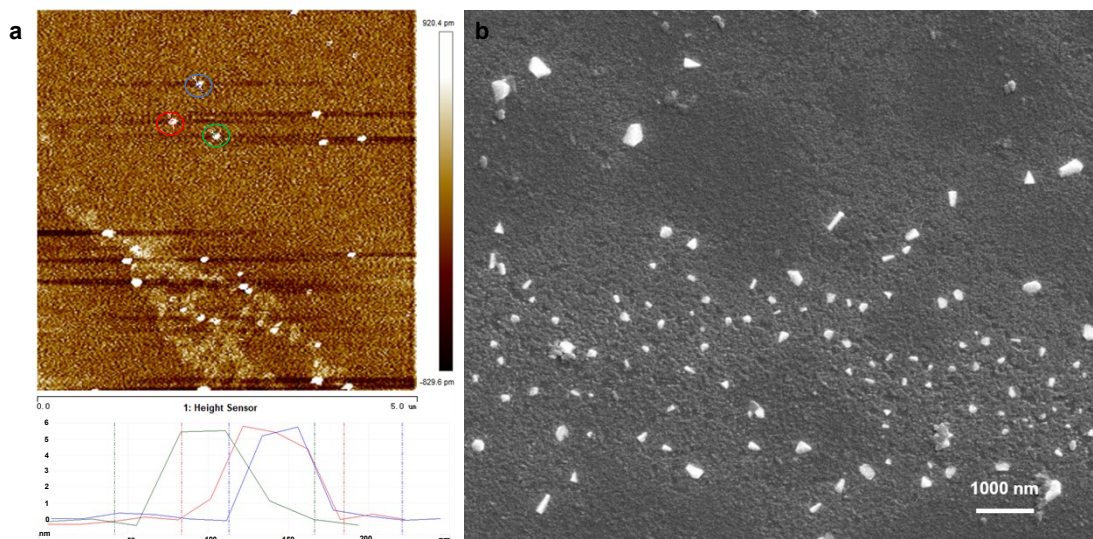


Figure S2. a) AFM height profile of thermodynamically stable Mn-TCPP aggregates. b) SEM image of the thermodynamically stable Mn-TCPP nanosheets. The SEM sample

was coated with Au before measurement.

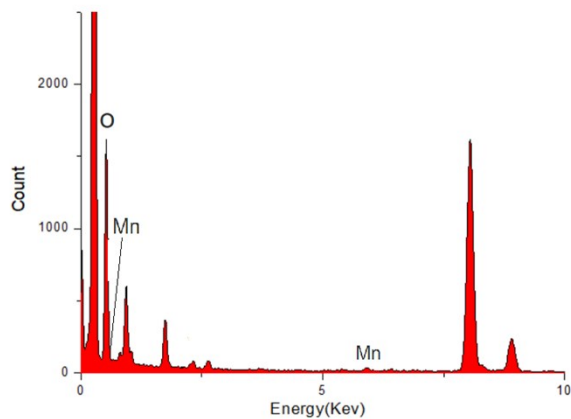


Figure S3. EDS profile of the thermodynamically stable Mn-TCPP nanosheets.

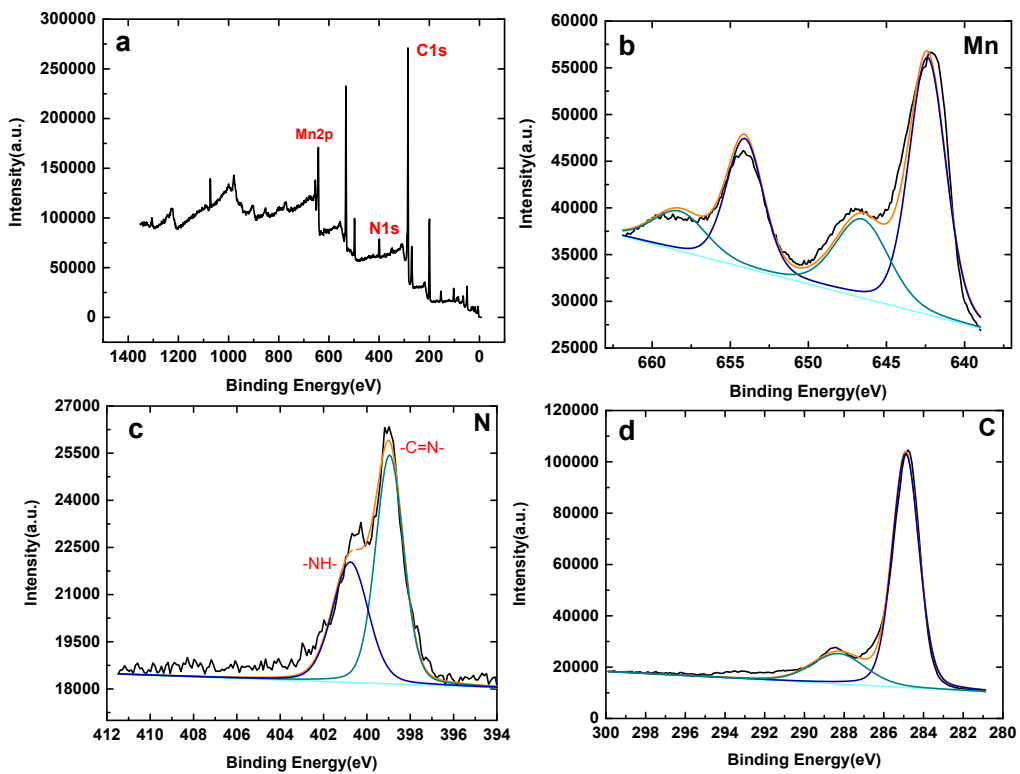


Figure S4. a) XPS analysis of thermodynamically stable Mn-TCPP nanosheets for b) Mn element, c) N element and d) C element.

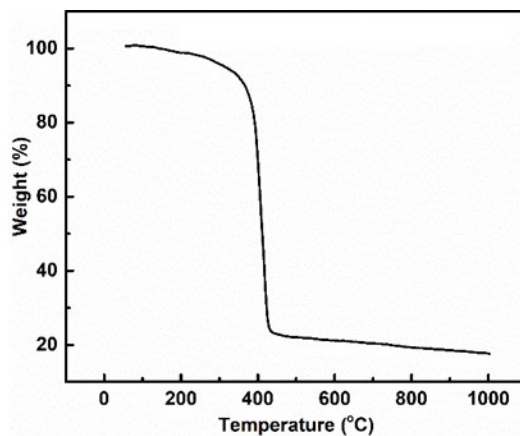


Figure S5. TG profile of thermodynamically stable Mn-TCPP nanosheets under Air atmosphere. (The TGA result showed that the MnO_2 content was about 20% which indicated that the Mn content in the Mn-TCPP nanosheets was calculated to be 12 wt%.)

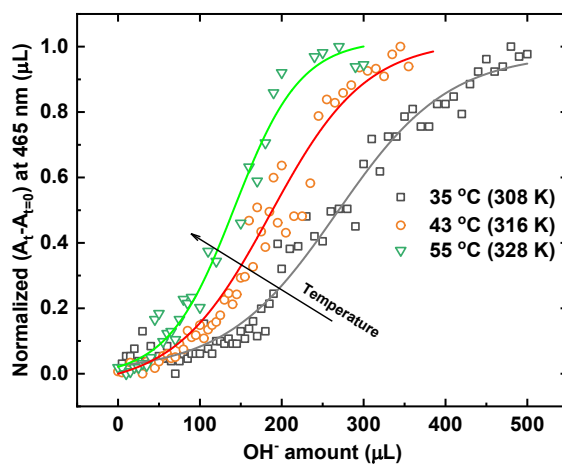


Figure S6. Temperature-dependent kinetic profile of absorption intensity at 465 nm of Mn/TCPP solutions versus additional OH^- amount ($[\text{OH}^-] = 10^{-2} \text{ M}$).

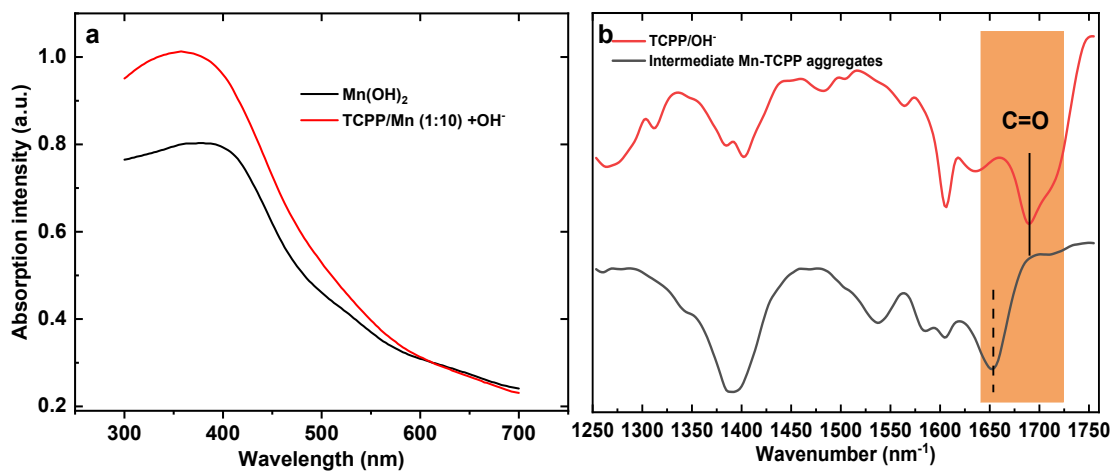


Figure S7. a) UV-Vis spectra of Mn(OH)_2 aqueous solution and suspension obtained from Mn/TCPP solutions (molar ratio: 1:10) under addition of OH^- (100 μL , $[\text{OH}^-] = 10^{-2}$ M) at 328 K. b) FT-IR spectra of TCPP/OH^- powder and intermediate Mn-TCPP aggregates.

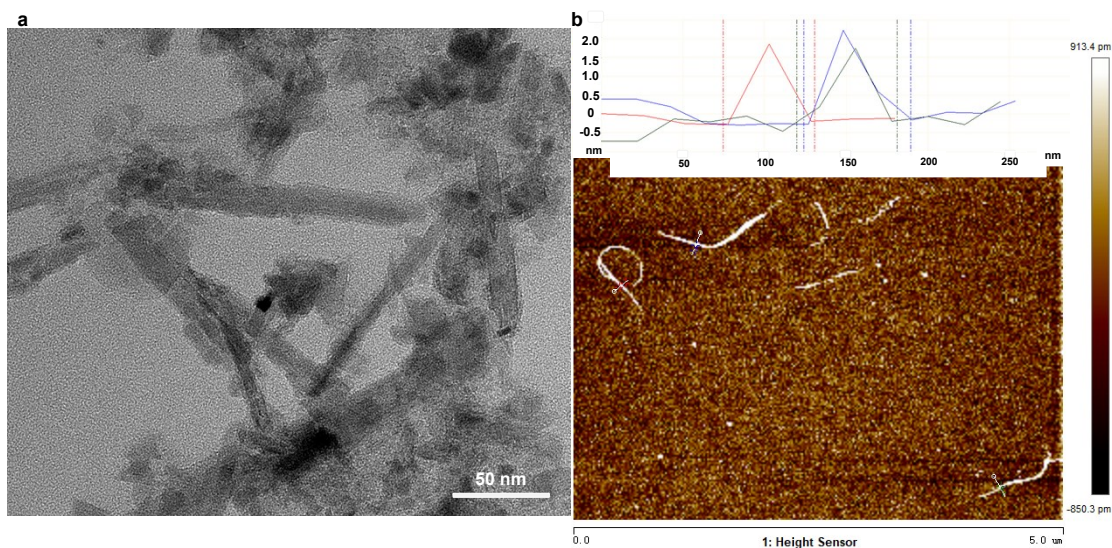


Figure S8. a) TEM image and b) AFM height profile of intermediate metastable Mn-TCPP aggregates.

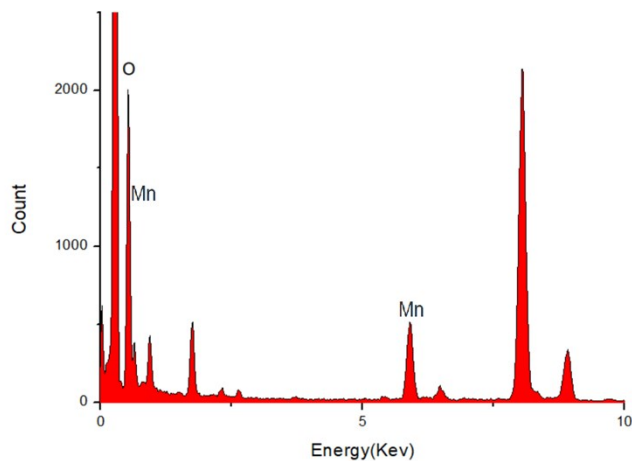


Figure S9. EDS profile of the intermediate Mn-TCPP tape structures.

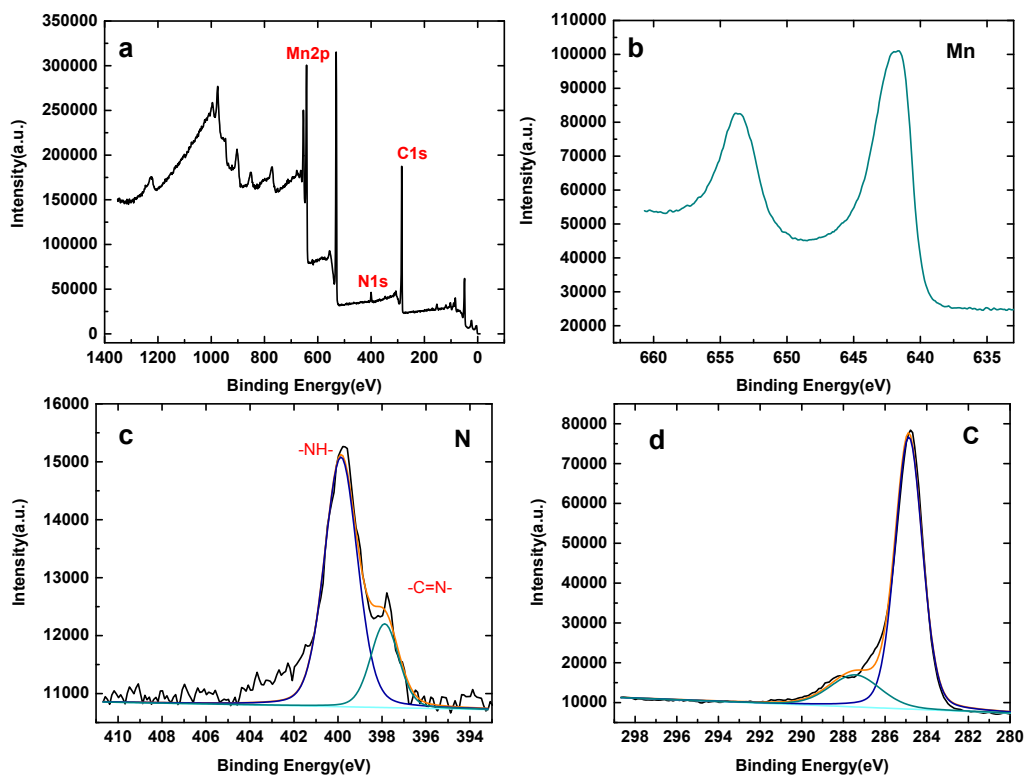


Figure S10. a) XPS analysis of intermediate metastable Mn-TCPP tape structures for b) Mn element, c) N element and d) C element.

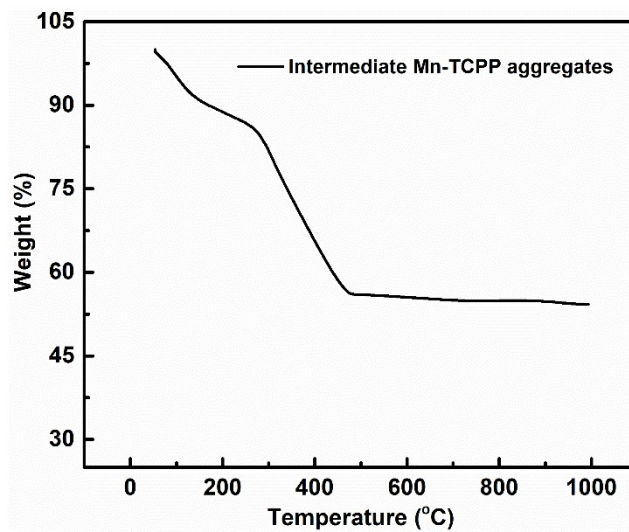


Figure S11. TG analysis profile of intermediate Mn-TCPP aggregates under Air atmosphere.

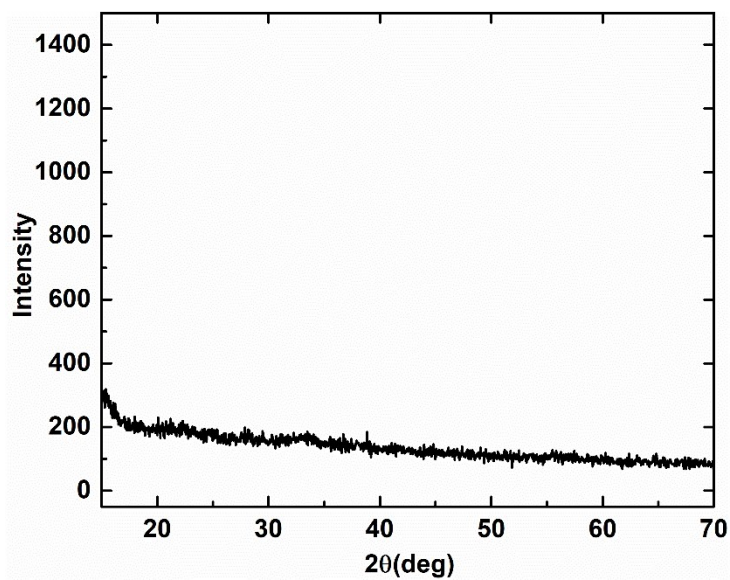


Figure S12. XRD profile of intermediate Mn-TCPP aggregates.

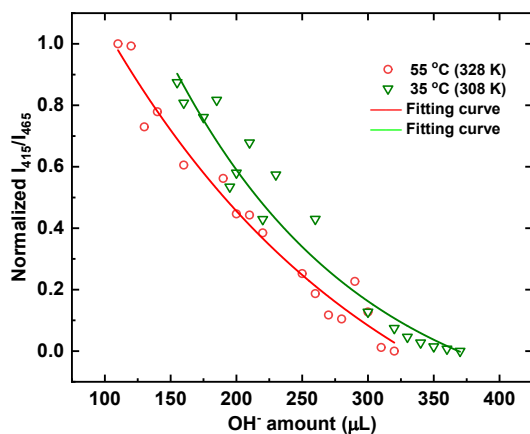


Figure S13. The absorption intensity ratio of I_{415}/I_{465} with additional OH^- amount ($[\text{OH}^-] = 10^{-2} \text{ M}$) in the phase II at 308 K and 328 K.

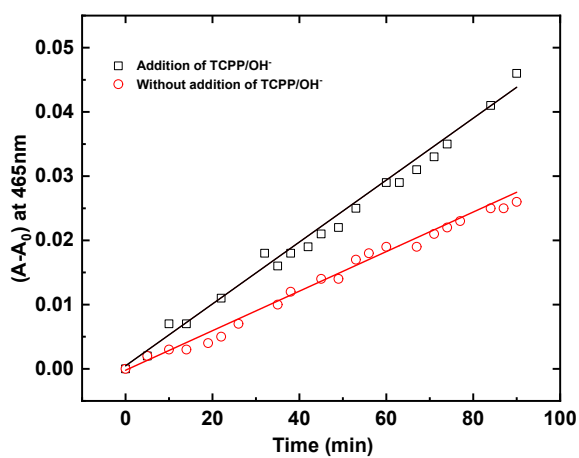


Figure S14. The plots of absorption intensity at 465 nm versus time with additional TCPP/ OH^- aqueous solution (black squares) and without TCPP/ OH^- aqueous solutions (red circles).

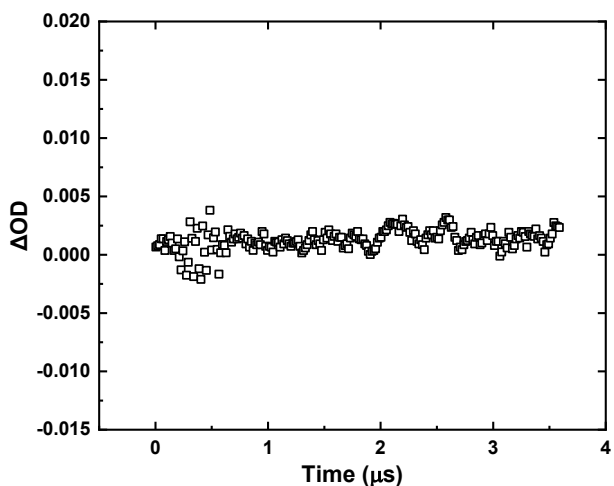


Figure S15. Transient absorbance spectrum of thermodynamically stable Mn-TCPP nanosheets in water at 460 nm under 355 nm laser pulse. All measurements are carried out at room temperature and N_2 atmosphere.

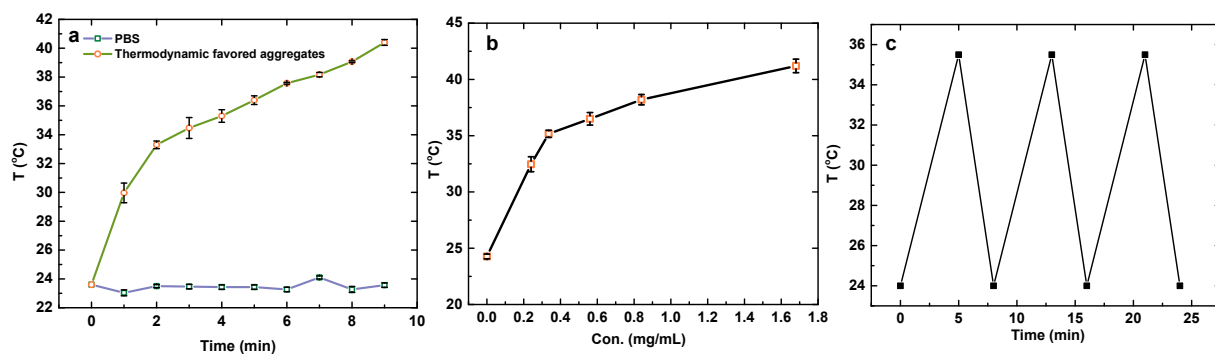


Figure S16. a) Temperature increase induced by thermodynamically stable Mn-TCPP aggregates (1.23 mg/mL) under light irradiation (637 nm, 200 mW/cm²). b) Concentration-dependent photothermal profile of thermodynamically stable Mn-TCPP aggregates upon light irradiation (637 nm, 200 mW/cm²). c) Photothermal stability test of thermodynamically stable Mn-TCPP aggregates (1.23 mg/mL) upon light irradiation (637 nm, 200 mW/cm²).